Bilge International Journal of Science and Technology Research

Web : http://dergipark.gov.tr/bilgesci **E-mail :** kutbilgescience@gmail.com

Received: 16.11.2017
Accepted: 07.03.2018
DOI: 10.30516/bilgesci.354763

ISSN: 2587-0742
e-ISSN: 2587-1749
2(1), 56-73, 2018

Experimental (FT-IR, Raman and NMR) and Theoretical (B3LYP, B3PW91, M06-2X and CAM-B3LYP) Analyses of P-Tert-Butylphenyl Salicylate

Nuri Öztürk[1*], Tuba Özdemir[2], Yelda Bingöl Alpaslan[3], Halil Gökce[4], Gökhan Alpaslan[4]

Abstract: The spectroscopic investigations of p-tert-butylphenyl salicylate ($C_{17}H_{18}O_3$) molecule were performed using ^{13}C and ^{1}H NMR chemical shifts, FT-IR and Raman spectroscopies. Molecular geometric optimizations, vibrational frequencies, Carbon-13 and Proton NMR chemical shifts (in vacuum and chloroform), HOMO-LUMO properties, natural bond orbital (NBO) analysis, nonlinear optical properties and thermodynamic parameters of p-tert-butylphenyl salicylate molecule was studied using B3LYP, B3PW91, M06-2X and CAM-B3LYP functionals in DFT method at the 6-311++G(d,p) basis set. NBO analysis was carried out to investigate the intramolecular hydrogen bonding (O-H···O) in the title molecule. Some of the molecular properties such as ionization potential (I), electron affinity (A), chemical hardness (η), chemical softness (ζ), electronegativity (χ), chemical potential (μ) and electrophilicity index (ω) parameters were determined via HOMO and LUMO energies of the title molecule. Also, quantum chemical computations were performed to determine the dipole moment (μ_{total}), mean polarizability (α), anisotropy of the polarizability ($\Delta\alpha$) and first hyperpolarizability (β_0) values. Thermochemical properties of the title molecule were investigated with the aforementioned calculation levels. The recorded experimental spectroscopic results were found to be in good agreement with the computed data.

Keywords: P-tert-butylphenyl salicylate, Vibrational spectroscopy, NMR chemical shifts, NLO properties, Thermodynamic properties, HOMO-LUMO analysis.

1. Introduction

P-tert-butylphenyl salicylate (TBS) is well-known commercial ultraviolet stabilizer and ultraviolet absorber (UVA). Ultraviolet absorbers (UVA) have been extensively studied due to the importance of protecting polymeric materials from photooxidation (Schmitt and Hirt, 1960; Gottfried and Dutzer, 1961; Newland and Tamblyn, 1964; Dobashi and Ohkatsu, 2008). As a salicylic acid derivative, 4-tert-butylphenyl salicylate (4-TBPS) exhibits anti-inflammatory activity. Choi et al. investigated the anti-inflammatory effects of 4-tert-butylphenyl salicylate (4-TBPS) (Choi et al., 2016). Salicylic acid derivatives are used for medicinal and cosmetic purposes. They are used as antipyretics, vitamins, antioxidants, NSAIDs, food preservatives, bactericidal agents, antiseptics, etc. (Hutchinson, 2003; Madan and Levitt, 2014). The molecular chemical formula and molecular weight of p-tert-butylphenyl salicylate are $C_{17}H_{18}O_3$ and 270.328 g/mol, respectively and its melting point is reported as 65-66 °C (Pubchem, 2017). Kasumov and Köksal studied new bidentate N-(2,5-di-tert-butylphenyl)salicylaldimines that involve X=H, HO, CH_3O, Br, NO_2, 3,5-di-Br, 3-NO_2-5-Br and

[1]Giresun University, Dereli Vocational School, 28950, Giresun, Turkey
[2]Bartın University, Vocational School of Health Services, 74100, Bartın, Turkey
[3]Giresun University, Faculty of Medicine, Department of Biophysics, 28100, Giresun, Turkey
[4]Giresun University, Vocational School of Health Services, 28200, Giresun, Turkey
Corresponding author: *nuri.ozturk@giresun.edu.tr

Citation: Öztürk, N., Özdemir, T., Alpaslan, Y.B., Gökçe, H., Alpaslan, G. (2018). Experimental (FT-IR, Raman and NMR) and Theoretical (B3LYP, B3PW91, M06-2X and CAM-B3LYP) Analyses of P-Tert-Butylphenyl Salicylate. Bilge International Journal of Science and Technology Research, 2(1), 56-73.

5,6-benzo substituents on the salicylaldehyde moiety, L_xH, and their mononuclear bis [N-(2,5-di-tertbutylphenyl) salicylaldiminato] copper (II) complexes, $Cu(L_x)_2$ using IR, UV-visible, ^1H NMR, ESR spectroscopy, magnetic measurements (Kasumov and Köksal, 2002). Raja et. al., investigated the molecular vibrations of 1-Naphthol in polycrystalline sample, at room temperature, using FT-IR and FT-Raman spectroscopy (Raja et al., 2013).

In this study, vibrational frequencies (FT-IR and Raman), NMR chemical shifts, optimized molecular geometric parameters, HOMO-LUMO analyses, NBO analysis, NLO properties and thermodynamic parameters of p-tert-butylphenyl salicylate were investigated both experimentally and theoretically. No detailed work was found on structural, spectral, electronic, nonlinear optical properties and thermodynamic investigations of the title molecule in the literature. The theoretical computations were performed using B3LYP, B3PW91, M06-2X and CAM-B3LYP functionals in DFT method with the 6-311++G(d,p) basis set. As theoretical analyses provide a powerful support for experimental studies, quantum chemical computations have been used by many researchers to determine the structural, spectroscopic, magnetic, electronic, optical and thermodynamic properties of the molecular systems in the literature (Buyukuslu et al., 2010; Ceylan et al., 2016; Kavitha and Velraj, 2016; Öztürk and Gökce, 2017).

2. Computational Details

Molecular geometric optimizations, vibrational wavenumbers, Proton and Carbon NMR chemical shifts (in vacuum and chloroform), NBO analysis, NLO properties, HOMO-LUMO analyses and thermodynamic parameters of the title molecule were studied using Gaussian 09W software package (Frisch et al., 2009). The calculated results were visualized via GaussView5.0 program (Dennington et al., 2009).

All quantum chemical computations were performed with B3LYP, B3PW91, M06-2X and CAM-B3LYP functionals in DFT method (Lee et al., 1988; Becke, 1993; Perdew et al., 1996; Yanai et al., 2004) at the 6-311++G(d,p) basis set in the ground state of the title molecule. The calculated harmonic vibrational wavenumbers were scaled with 0.9671 for B3LYP/6-311++G(d,p) level, 0.9576 for B3PW91/6-311++G(d,p) level, 0.9489 for M06-2X/6-311++G(d,p) level and 0.9665 for CAM-B3LYP/6-311++G(d,p) level (Cruz et al., 2015; Kanagathara et al., 2015; Chase et al., 2016).

Using optimized molecular geometries, ^1H and ^{13}C NMR isotropic chemical shift were computed with aforementioned computational levels using integral equation formalism polarizable continuum model (IEFPCM), solvent model and gauge invariant atomic orbital (GIAO) approach (London, 1937; Ditchfield, 1974; Wolinski et al., 1990). The HOMO and LUMO analyses were performed using aforementioned computational levels. According to HOMO and LUMO energy values, the quantum molecular descriptors such as ionization potential (I), electron affinity (A), chemical hardness (η), chemical softness (ζ), electronegativity (χ), chemical potential (μ) and electrophilicity index (ω) parameters were computed. Nonlinear optical (NLO) properties such as dipole moment (μ), mean polarizability (α_{total}), anisotropy of the polarizability ($\Delta\alpha$) and first hyperpolarizability (β_0) were computed with the mentioned computational levels. NBO analysis was performed to investigate the intramolecular hydrogen bonding interaction (O-H···O) in the title compound molecule. Finally, thermodynamic properties (thermal energy (E), heat capacity (C_v), entropy (S), zero-point energy, etc.) were calculated at B3LYP, B3PW91, M06-2X and CAM-B3LYP/6-311++G(d,p) levels.

3. Results and Discussion

3.1. Molecular structure analysis

The optimized molecular structure of p-tert-butylphenyl salicylate was given in Figure 1 with numbering of the atoms. The optimized molecular geometric parameters including bond lengths and angles, as given in Table 1, were calculated using B3LYP, B3PW91, M06-2X and CAM-B3LYP/6-311++G(d,p) theoretical methods.

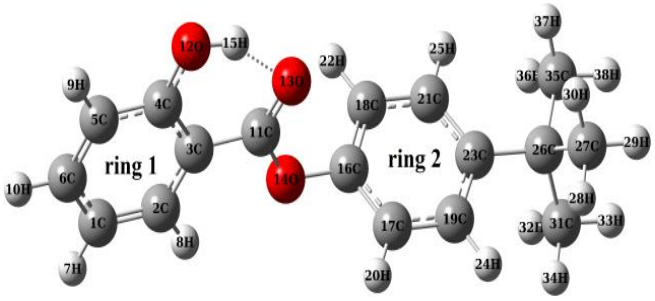

Figure 1. The optimized molecular structure with the B3LYP/6-311++G(d,p) level of p-tert-butylphenyl salicylate

Table 1. The optimized molecular geometric parameters of p-tert-butylphenyl salicylate.

Bond lengths (Å)	B3LYP	B3PW91	M06-2X	CAM-B3LYP	Bond angles (°)	B3LYP	B3PW91	M06-2X	CAM-B3LYP
C1-C2	1.383	1.381	1.380	1.377	C2-C1-C6	119.3	119.3	119.2	119.2
C1-C6	1.402	1.400	1.399	1.397	C1-C2-C3	121.0	120.9	120.9	120.9
C2-C3	1.407	1.404	1.403	1.401	C2-C3-C4	119.2	119.4	119.5	119.4
C3-C4	1.417	1.415	1.409	1.408	C2-C3-C11	122.0	122.1	121.6	121.8
C3-C11	1.469	1.465	1.473	1.467	C4-C3-C11	118.7	118.5	118.9	118.8
C4-C5	1.402	1.400	1.399	1.397	C3-C4-O12	123.0	122.9	123.5	123.0
C4-O12	1.344	1.337	1.339	1.338	C5-C4-O12	117.7	118.0	117.3	117.7
C5-C6	1.385	1.382	1.381	1.378	C4-C5-C6	120.3	120.2	120.3	120.2
C11-O13	1.221	1.220	1.212	1.215	C1-C6-C5	120.9	121.0	121.0	121.0
C11-O14	1.356	1.350	1.347	1.346	C3-C11-O13	124.3	124.2	124.4	124.2
O14-C16	1.405	1.398	1.395	1.399	C3-C11-O14	113.3	113.4	112.9	113.5
C16-C17	1.388	1.386	1.386	1.382	O13-C11-O14	122.4	122.4	122.8	122.3
C16-C18	1.385	1.383	1.382	1.378	C4-O12-H15	107.9	107.2	108.7	108.2
C17-C19	1.391	1.389	1.388	1.385	C11-O14-C16	119.0	118.7	119.4	118.5
C18-C21	1.395	1.392	1.392	1.390	O14-C16-C17	118.4	118.3	117.2	118.8
C19-C23	1.403	1.401	1.399	1.397	O14-C16-C18	120.7	120.7	121.7	120.1
C21-C23	1.400	1.397	1.396	1.393	C17-C16-C18	120.9	120.9	121.1	121.0
C23-C26	1.539	1.533	1.530	1.532	C16-C17-C19	119.2	119.1	119.1	119.1
C26-C27	1.547	1.540	1.538	1.538	C16-C18-C21	119.2	119.2	119.0	119.2
C26-C31	1.547	1.540	1.538	1.538	C17-C19-C23	121.8	121.8	121.6	121.8
C26-C35	1.540	1.533	1.532	1.532	C18-C21-C23	121.8	121.8	121.7	121.6
O13···H15	1.752	1.720	1.788	1.745	C19-C23-C21	117.2	117.2	117.5	117.4
O12···O13	2.619	2.598	2.635	2.608	C19-C23-C26	119.9	119.9	119.7	119.8
					C21-C23-C26	122.9	122.9	122.9	122.8
					C23-C26-C27	109.4	109.3	109.4	109.4
					C23-C26-C31	109.5	109.4	109.2	109.4
					C23-C26-C35	112.3	112.2	112.1	112.2
					C27-C26-C31	109.4	109.4	109.4	109.4
					C27-C26-C35	108.1	108.2	108.3	108.2
					C31-C26-C35	108.2	108.2	108.3	108.2
					O12-H15···O13	145.3	146.6	143.5	144.9

The calculated molecular geometric parameters were compared with the experimental and theoretical geometric parameters of similar structures in the literature (Bilgram et al., 1982; Hammond et al., 2002; Hanuza et al., 2004). C11-O14 and C11=O13 bond lengths in the salicylate group of the title compound were computed as 1.356 Å, 1.350 Å, 1.347 Å, 1.346 Å and 1.221 Å, 1.220 Å, 1.212 Å, 1.215 Å respectively, using B3LYP, B3PW91, M06-2X, CAM-B3LYP/6-311++G(d,p) levels. Likewise, the C4-O12 bond length was found as 1.344 Å for B3LYP, 1.337 Å

for B3PW91, 1.339 Å for M06-2X and 1.338 Å. C11-O14, C11=O13 and C4-O12 bond lengths for salol (phenyl salicylate or benzoic acid 2-hydroxyphenylester) molecule were reported as 1.354 Å, 1.215 Å and 1.356 Å with experimental X-Ray analysis by Bilgram et al. (Bilgram et al., 1982), respectively. For salol molecule, Hanuza et al. (Hanuza et al., 2004) calculated C11-O14 bond length as 1.349 Å, C11=O13 bond length as 1.224 Å and C4-O12 bond length as 1.333 Å using MPW1PQ91/6-31G(d,p) level. Similarly, Hammond et al. (Hammond et al., 2002) reported the molecular structure and molecular geometric parameters of salol molecule in meta-stable phase using X-Ray powder diffraction analysis. C3-C11 and C16-O14 bond lengths were respectively found as 1.469 Å, 1.465 Å, 1.473 Å, 1.467 Å and 1.405 Å, 1.398 Å, 1.395 Å, 1.399 Å with the aforementioned computational methods. Experimental values of these bond lengths were reported as 1.464 Å and 1.411 Å, respectively (Bilgram et al., 1982). The C-C bond lengths in ring 1 and ring 2 of the title compound were calculated at the interval of 1.383-1.417 Å and 1.385-1.403 Å for B3LYP, 1.381-1.415 Å and 1.383-1.401 Å for B3PW91, 1.380-1.409 Å and 1.382-1.399 Å for M06-2X and 1.377-1.408 Å and 1.378-1.397 Å for CAM-B3LYP, respectively. The hydrogen bonding parameters for O12-H15, O13···H15, O12···O13 and O12-H15···O13 were computed as 0.982 Å, 1.752 Å, 2.619 Å and 145.3° for B3LYP, 0.983 Å, 1.720 Å, 2.598 Å and 146.6° for B3PW91, 0.974 Å, 1.788 Å, 2.635 Å and 143.5° for M06-2X and 0.979 Å, 1.745 Å, 2.608 Å and 144.9° for CAM-B3LYP. C3-C11-O13, O13-C11-O14, C4-O12-H15 and C11-O14-C16 bond angles were computed as 124.3°, 122.4°, 107.9° and 119.0° for B3LYP, 124.2°, 122.4°, 107.2° and 118.7° for B3PW91, 124.4°, 122.8°, 108.7° and 119.4° for M06-2X and 124.2°, 122.3°, 108.2° and 118.5° for CAM-B3LYP, whereas their experimental values were reported as 125.1°, 121.9°, 105.7° and 117.6°, respectively (Bilgram et al., 1982). C4-C3-C11-O14, C3-C11-O14-C16, C11-O14-C16-C17 and C19-C23-C26-C31 dihedral angle values were calculated as 179.5°, 179.4°, 109.1° and 60.0° for B3LYP, 179.4°, 179.1°, 110.3° and 60.0° for B3PW91, -180.0°, -179.9°, 124.7° and 60.7° for M06-2X and 179.8°, -180.0°, 101.2° and 59.9° for CAM-B3LYP, respectively.

We can see from computed vibrational wavenumbers given in Table 2 that imaginary frequency value is not found at B3LYP, B3PW91 and M06-2X/6-311++G(d,p) levels, whereas one imaginary frequency value (mode no:ν_1= -3.2 cm^{-1}) is computed at CAM-B3LYP/6-311++G(d,p) level. This situation shows that the minimum energy state in the available conformation was not achieved for CAM-B3LYP/6-311++G(d,p) level. This molecular structure is an unstable conformational form for CAM-B3LYP/6-311++G(d,p) level and it can be a saddle point or transition state or non-minimum energy point over PES of the title compound. The vibrational assignment corresponding to this vibrational mode (mode no: ν_1) in all computational methods is torsional mode ($\tau C_{11}O_{14}C_{16}C_{17}$) between salicylate group and p-tert-butylphenyl group in the title compound.

3.2. Vibrational frequency analysis

P-tert-butylphenyl salicylate molecule has 38 atoms and 108 fundamental vibrational modes. The recorded (AIST, 2017) and calculated vibrational wavenumbers, IR intensities, Raman scattering activities and vibrational assignments were summarized in Table 2. The recorded (AIST, 2017) and calculated IR and Raman spectra of the title molecule were presented in Figures. 2 and 3, respectively. The OH, CH, CC, C-O and C=O vibrational results obtained with experimental and computational methods are in good agreement with the results given in the literature (Nyquist et al., 1996; Kalampounias et al., 2003; Baran and Davydova, 2010). The linear correlation coeffections (R^2) between experimental and computed vibrational wavenumbers were also given in Table 2.

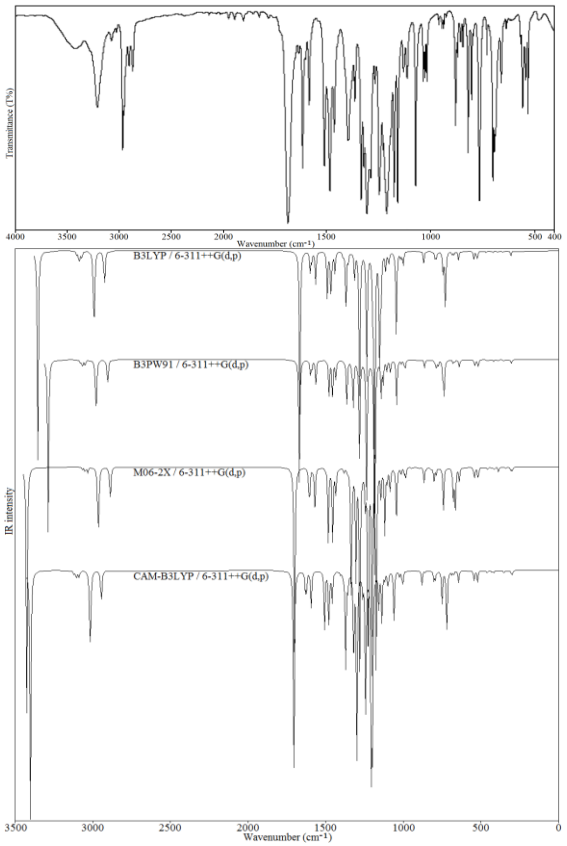

Figure 2. The experimental (AIST, 2017) (top) and simulated (bottom) IR spectra of p-tert-butylphenyl salicylate.

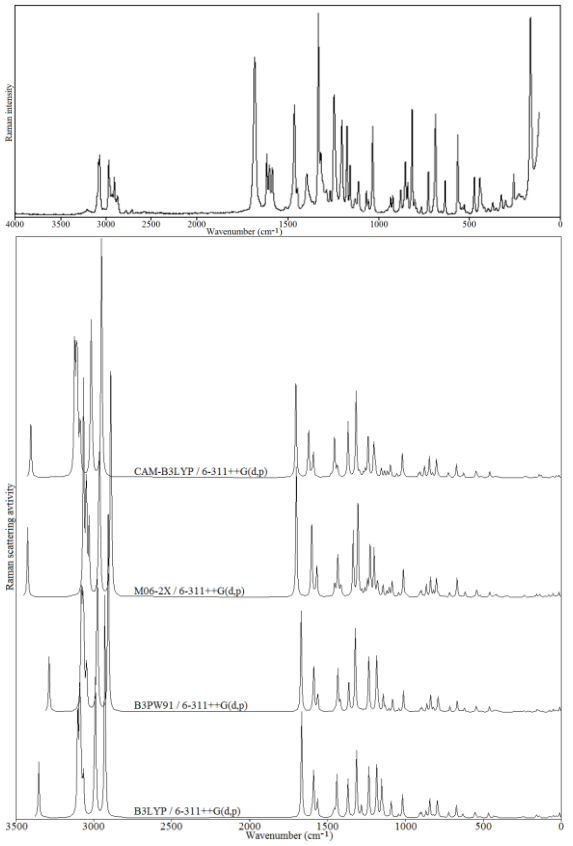

Figure 3. The experimental (AIST, 2017) (top) and simulated (bottom) Raman spectra of p-tert-butylphenyl salicylate.

The OH vibrations are very sensitive due to effect of hydrogen bonding and the OH stretching modes observe in the region of 2800-3250 cm^{-1} (Colthup et al., 1964; Bellamy, 1975). Due to O12-H15···O13 intramolecular hydrogen bonding in the title molecule, the OH stretching band was observed at 3207 cm^{-1} in IR spectrum and 3208 cm^{-1} in Raman spectrum. This stretching band was computed at 3353.0 cm^{-1} with B3LYP, 3286.9 cm^{-1} with B3PW91, 3424.6 cm^{-1} with M06-2X and 3401.3 cm^{-1} with CAM-B3LYP. OH in-plane bending modes were observed and computed as mixed with other vibrations in the region of 1200-1600 cm^{-1}. However, the OH out-of-plane bending mode was obtained as individual bands. The OH out-of-plane bending bands were not observed in IR and Raman spectra of the title molecule. These bands were computed at 728.2 (mode no:ν_{35}) and 775.6 (mode no:ν_{37}) cm^{-1} with B3LYP, 744.3 (mode no:ν_{36}) and 773.7 (mode no:ν_{37}) cm^{-1} with B3PW91, 663.9 (mode no:ν_{32}) and 677.2 (mode no:ν_{34}) cm^{-1} with M06-2X and 727.5 (mode no:ν_{34}) and 791.1 (mode no:ν_{37}) cm^{-1} with CAM-B3LYP.

The aromatic CH stretching vibrational modes occur in the region of 3000-3100 cm^{-1} (Colthup et al., 1964; Bellamy, 1975; Silverstein and Webster, 1998; Stuart, 2004). The bands recorded at 3023, 3068 and 3073 cm^{-1} in IR and Raman spectra of the title compound can be attributed to the aromatic CH stretching modes. These modes were computed at the interval of 3065.4-3104.3 cm^{-1} for B3LYP, 3045.2-3081.7 cm^{-1} for B3PW91, 3029.7-3066.4 cm^{-1} for M06-2X and 3086.2-3123.6 cm^{-1} for CAM-B3LYP. Symmetric and asymmetric stretching modes for methyl and methylene groups were observed between 2800 cm^{-1} and 3000 cm^{-1} (Colthup et al., 1964; Bellamy, 1975; Silverstein and Webster, 1998; Stuart, 2004). As seen in Table 2, CH_3 symmetric stretching bands were appeared at 2869 and 2900 cm^{-1} in IR spectrum and at 2872, 2905 and 2932 cm^{-1} in Raman spectrum and the corresponding calculated scaled frequencies were computed in the regions of 2921.5-2929.3 cm^{-1}, 2900.6-2907.4 cm^{-1}, 2883.8-2891.3 cm^{-1}, 2944.1-2951.2 cm^{-1} with B3LYP, B3PW91, M06-2X and CAM-B3LYP functionals using 6-311++G(d,p)

basis set, respectively. Similarly, the asymmetric CH_3 stretching modes were observed at 2969 (IR)-2968 (R) cm^{-1} and computed in the region 2981.6-2996.6 cm^{-1} for B3LYP, 2970.1-2983.8 cm^{-1} for B3PW91, 2956.4-2969.0 cm^{-1} for M06-2X and 3008.1-3022.1 cm^{-1} for CAM-B3LYP. The other vibrational modes (in-plane bending, out-of-plane bending, rocking, scissoring and symmetric bending) of the aromatic and methyl groups in the title compound were summarized in Table 2.

Carbonyl (C=O) groups cause strong C=O stretching absorption bands in the region of 1540-1870 cm^{-1} in IR and Raman spectra (Silverstein and Webster, 1998). The peak at 1686 (IR)-1681 (R) cm^{-1}, observed as a strong band in IR and Raman spectra of the title compound, can be assigned to C=O stretching mode. This mode was calculated at 1665.6 cm^{-1} for B3LYP, 1669.1 cm^{-1} for B3PW91, 1699.6 cm^{-1} for M06-2X and 1709.6 cm^{-1} for CAM-B3LYP. The C4-O12 stretching mode in phenolic group of the title compound was obtained in mode no: $\nu_{66,}$ ν_{68} and ν_{69} with B3LYP, mode no: $\nu_{66,}$ ν_{67} and ν_{69} with B3PW91, mode no: $\nu_{66,}$ ν_{70} and ν_{71} with M06-2X and mode no: $\nu_{66,}$ ν_{70} and ν_{71} with CAM-B3LYP. Likewise, the C11-O14 stretching mode was observed at 1057 cm^{-1} in Raman spectrum and it is calculated at 1044.1, 1041.7, 1043.0 and 1066.8 cm^{-1} with all mentioned computational levels (mode no: ν_{56}). Additionally, C16-O14 stretching mode was found at mode no: ν_{64} with B3LYP, mode no: ν_{64} with B3PW91, mode no: ν_{65} with M06-2X level and mode no: ν_{65} with CAM-B3LYP.

The C23-C26 and C3-C11 stretching modes were observed at 1247 (IR)-1243 (R) cm^{-1} (mode no:ν_{67}) and 1304 (IR)-1307 (R) cm^{-1} (mode no:ν_{71}), respectively and they were computed at 1240.0 cm^{-1} and 1313.0 cm^{-1} for B3LYP, 1236.6 cm^{-1} and 1321.2 cm^{-1} for B3PW91, 1243.3 cm^{-1} and 1304.2 cm^{-1} for M06-2X level and 1267.7 cm^{-1} and 1326.2 cm^{-1} for CAM-B3LYP. The vibrations in aromatic groups and other groups of the title molecule were summarized in Table 2.

Table 2. The experimental (AIST, 2017) and computed vibrational wavenumbers and their assignments of p-tert-butylphenyl salicylate.

Mode	Assignments	Exp. freq. (cm^{-1})		B3LYP/6-311++G(d,p)			B3PW91/6-311++G(d,p)			M06-2X/6-311++G(d,p)			CAM-B3LYP/6-311++G(d,p)		
		IR	Raman	Freq.	I_{IR}	S_{Raman}	Freq.	I_{IR}	S_{Raman}	Freq.	I_{IR}	S_{Raman}	Freq.	I_{IR}	S_{Raman}
ν_1	Lattice mode	-	-	10.3	0.30	6.00	9.5	0.30	5.85	13.2	0.44	3.85	-3.2	0.26	6.26
ν_2	Lattice mode	-	-	27.8	0.37	2.05	27.5	0.37	2.07	24.6	0.23	1.28	28.9	0.37	2.09
ν_3	Lattice mode	-	-	37.0	0.47	0.69	37.7	0.47	0.68	39.5	0.37	0.73	34.7	0.51	0.47
ν_4	Lattice mode	-	-	49.3	0.03	2.95	49.5	0.03	3.11	52.1	0.02	3.33	48.1	0.02	1.80
ν_5	Lattice mode	-	-	74.0	0.07	1.82	74.5	0.09	1.97	79.4	0.15	2.09	73.3	0.03	1.33
ν_6	$\delta C_{23}C_{26}C_{27,31,35}+\delta C_{16}O_{14}C_{11}$	-	-	103.2	0.13	0.79	102.0	0.12	0.75	102.0	0.07	0.71	104.5	0.18	0.81
ν_7	τring1+$\tau O_{13}C_{11}C_3C_2$	-	-	140.4	0.01	2.33	139.9	0.02	2.29	137.8	0.01	2.81	143.5	0.02	2.28
ν_8	$\delta O_{14}C_{11}C_3+\delta C_{16}O_{14}C_{11}$	-	160	156.2	0.81	3.59	154.7	0.79	3.41	157.3	0.80	2.68	157.5	0.73	3.24
ν_9	$\delta C_{21}C_{23}C_{26}+\delta C_{23}C_{26}C_{35}+\delta C_{17}C_{16}O_{14}$	-	-	196.6	0.02	0.44	193.1	0.02	0.47	194.5	0.07	0.48	201.0	0.01	0.30
ν_{10}	τCH_3	-	207	214.1	0.02	0.87	212.0	0.03	0.86	203.5	0.10	0.32	212.0	0.07	0.50
ν_{11}	$\tau CH_3+\tau$ring1	-	225	239.0	0.32	1.04	237.3	0.27	1.05	233.5	0.37	1.60	240.7	0.40	1.22
ν_{12}	$\tau CH_3+\tau$ring1	-	-	242.9	0.29	0.87	240.6	0.43	0.81	242.5	0.59	0.61	245.7	0.06	0.97
ν_{13}	τCH_3	-	255	267.7	0.28	0.04	266.6	0.27	0.04	263.7	0.35	0.05	266.9	0.18	0.06
ν_{14}	$\tau CH_3+\delta C_{11}C_3C_4$	-	302	304.2	7.20	0.09	301.8	7.56	0.29	296.4	5.07	0.84	307.1	6.13	0.36
ν_{15}	$\delta C_{27}C_{26}C_{31}+\tau CH_3$	-	-	306.4	1.07	0.88	302.4	3.09	0.89	305.1	5.19	0.51	313.6	4.96	0.53
ν_{16}	τCH_3	-	323	308.6	3.05	0.29	306.9	0.63	0.12	323.4	0.12	0.04	320.8	0.14	0.03
ν_{17}	δC-CH_3 (sym. bendig)	-	353	342.4	1.67	0.87	337.8	1.98	0.80	341.0	1.72	1.38	346.5	1.32	0.90
ν_{18}	$\delta C_{27}C_{26}C_{35}+\delta C_{31}C_{26}C_{35}$	-	370	358.8	3.52	0.32	351.2	3.60	0.31	356.8	1.78	0.32	361.5	4.37	0.28
ν_{19}	$\delta C_{17}C_{16}O_{14}+\delta C_{27}C_{26}C_{31}+\tau$ring2	-	396	392.4	3.30	0.05	387.4	3.74	0.04	386.2	7.37	0.11	398.2	2.00	0.03
ν_{20}	τring2	-	-	409.6	0.09	0.72	403.5	0.08	0.83	403.4	0.15	0.42	415.3	0.25	0.10
ν_{21}	$\delta O_{13}C_{11}C_3+\tau$ring2+$\tau$ring1	-	416	420.5	3.67	1.59	416.4	4.70	1.27	414.0	3.67	2.01	425.4	4.14	1.59
ν_{22}	τring1+$\tau O_{13}C_{11}O_{14}C_{16}+\delta C_{27}C_{26}C_{31}$	-	428	428.1	0.44	0.61	422.9	0.20	0.65	419.2	0.21	1.30	434.5	0.58	0.32
ν_{23}	$\delta C_{27}C_{26}C_{31}+\tau$ring2+$\tau$ring1	-	442	434.1	1.53	1.87	429.2	1.49	2.11	431.0	1.89	1.34	439.4	2.67	1.25
ν_{24}	$\delta C_{26}C_{23}C_{31}+\delta O_{14}C_{16}C_{17}+\delta C_{27}C_{26}C_{31}$	-	-	461.0	0.67	0.36	455.0	0.61	0.32	451.9	1.08	0.56	466.9	0.66	0.31
ν_{25}	$\delta O_{12}C_4C_3+\delta$C-$CH_3$ (sym. bending)	471	470	466.1	3.81	6.40	461.0	3.54	7.10	458.2	3.48	4.75	470.9	3.73	6.34
ν_{26}	τring1+$\gamma C_3O_{12}C_5C_4$	-	-	520.4	8.36	0.18	514.7	8.93	0.19	514.3	8.03	0.19	529.6	8.90	0.13
ν_{27}	δC-CH_3 (sym. bending)+δring2+$\delta O_{12}C_4C_5$	525	527	524.8	11.15	1.41	518.2	12.52	1.06	519.1	12.47	1.41	530.7	12.10	1.41
ν_{28}	$\gamma C_{19}C_{21}C_{26}C_{23}+\gamma C_{17}C_{18}O_{14}C_{16}+$ τHCCC in ring 2	536	538	544.4	16.88	2.08	537.8	16.61	2.04	539.5	12.81	4.86	552.6	17.31	2.23
ν_{29}	[τHCCC+τCCCC]in ring 2+δring1	554	562	552.8	1.08	7.59	545.8	1.18	7.43	544.7	6.57	4.11	559.4	1.36	6.71
ν_{30}	δring2	630	633	630.8	0.68	5.55	621.1	0.57	5.54	615.6	0.71	5.58	637.5	0.21	5.61
ν_{31}	$\nu C_{23}C_{26}+\delta$ring2+δring1+$\delta O_{13}C_{11}C_3$	654	657	643.9	18.48	1.97	638.6	21.07	1.34	638.4	21.95	1.18	652.7	21.16	1.39
ν_{32}	[τHCCC+τCCCC] in ring 2+$\nu C_{26}C_{27,31,35}$	684	685	672.3	7.06	16.58	667.5	5.94	16.21	663.9	63.47	1.02	683.2	6.14	14.74
ν_{33}	$\gamma C_3O_{13}O_{14}C_{11}+\gamma O_{12}C_3C_5C_4+\tau$HCCC in ring 1	694	-	684.1	7.66	0.33	678.3	10.11	0.35	668.3	4.76	18.51	696.8	6.57	0.19
ν_{34}	τring2	723	724	720.6	5.10	8.14	714.4	2.73	7.58	677.2	48.64	0.18	727.5	106.45	0.44
ν_{35}	τHOCC	-	-	728.2	109.89	0.81	735.5	90.03	0.32	716.4	1.88	4.98	734.9	3.39	6.11
ν_{36}	τHCCC in ring 1+τHOCC+$\gamma O_{12}C_3C_5C_4+$ $\gamma O_{13}O_{14}C_3C_{11}$	760	764	743.4	40.19	0.23	744.3	47.14	0.56	740.1	67.55	0.20	757.9	56.71	0.25
ν_{37}	$\gamma C_3O_{13}O_{14}C_{11}+\tau$HOCC+$\tau$HCCC in ring 1	-	-	775.6	3.22	0.53	773.7	15.32	0.41	770.0	1.10	0.57	791.1	2.47	0.57

ν_{38}	δring2+δring1+$\nu C_{26}C_{27,31,35}$+$\delta O_{13}C_{11}C_3$	790	790	786.5	12.78	3.68	784.6	15.84	5.83	787.0	11.23	2.92	801.7	14.53	3.50
ν_{39}	τHCCC in ring 2+$\delta O_{13}C_{11}O_{14}$	-	-	794.8	13.58	25.57	790.5	12.70	18.93	800.7	22.32	19.84	811.2	16.59	20.68
ν_{40}	τHCCC in ring 2	797	800	806.8	1.45	0.70	798.8	3.59	1.41	807.4	2.27	0.46	822.0	0.34	0.07
ν_{41}	ρCH_3+$\nu C_{26}C_{27,31,35}$+$\nu C_{26}C_{23}$+ τHCCC in ring 2	816	815	820.6	0.69	4.00	818.5	0.57	5.35	820.0	2.53	6.12	836.3	0.33	4.54
ν_{42}	δring1+δring2+$\nu O_{14}C_{16}$	839	838	842.8	1.03	26.83	837.5	0.48	24.66	838.4	0.26	19.45	856.3	0.33	23.55
ν_{43}	[τHCCC+τCCCC] in ring 1	851	850	848.7	2.22	0.05	838.9	1.65	0.97	852.3	3.01	0.03	866.9	2.80	0.05
ν_{44}	τHCCC in ring 2+$\gamma O_{14}C_{17}C_{18}C_{16}$+ $\delta O_{14}C_{11}O_{13}$+$\delta$CCC in ring 1	864	-	867.5	26.06	9.71	862.0	22.59	10.98	865.2	23.44	12.35	887.2	25.18	13.08
ν_{45}	ρCH_3+$\nu C_{27,31,35}C_{26}$	876	878	896.6	1.99	7.43	893.5	1.82	6.01	897.2	1.54	6.04	913.8	2.18	6.06
ν_{46}	ρCH_3+$\nu C_{27,31,35}C_{26}$	-	-	906.4	0.53	6.14	902.2	1.03	4.87	905.8	1.23	4.80	924.8	0.92	4.97
ν_{47}	ρCH_3+τHCCC in ring 2	921	923	929.3	0.38	0.35	912.3	0.22	0.21	910.6	0.33	0.14	935.9	0.13	0.03
ν_{48}	τHCCC in ring 2+ρCH_3	932	935	933.6	0.46	0.32	921.3	0.71	0.62	930.9	0.70	0.81	954.8	0.75	1.22
ν_{49}	τHCCC in ring 1	940	-	943.6	0.93	0.09	932.4	0.93	0.07	946.0	0.05	0.12	967.0	0.02	0.05
ν_{50}	τHCCC in ring 2	-	-	945.6	0.03	0.27	934.9	0.02	0.32	948.6	1.41	0.10	967.9	0.88	0.09
ν_{51}	τHCCC in ring 1	956	-	963.1	0.09	0.01	951.1	0.08	0.01	964.7	0.11	0.01	989.0	0.11	0.01
ν_{52}	δring2+ρCH_3	-	-	998.4	24.70	0.41	986.3	21.81	0.48	983.4	16.63	0.52	1009.3	20.75	0.54
ν_{53}	ρCH_3	1013	-	1007.8	9.97	1.39	993.9	11.18	1.40	992.6	8.10	1.46	1016.3	11.11	1.22
ν_{54}	ρCH_3	1024	-	1014.9	0.05	1.24	999.1	0.23	1.27	999.6	0.03	1.34	1022.8	0.02	1.39
ν_{55}	[δCCC+νCC] in ring 1	1033	1032	1017.9	10.69	32.23	1012.1	10.20	30.16	1013.1	10.07	31.82	1031.8	10.53	29.91
ν_{56}	$\nu O_{14}C_{11}$+δring1	-	1057	1044.1	163.32	5.08	1041.7	118.31	4.71	1043.0	82.70	4.60	1066.8	87.65	4.87
ν_{57}	[δHCC+νCC+δCCC] in ring 2+ $\nu C_{23}C_{26}$+ρCH_3	1067	1066	1090.9	18.80	24.22	1082.0	24.67	19.45	1080.2	9.02	0.63	1102.1	12.03	3.25
ν_{58}	δHCC in ring 2	-	-	1096.7	7.17	0.14	1083.9	10.04	1.27	1084.8	29.11	17.39	1107.5	21.12	14.30
ν_{59}	[δHCC+νCC] in ring 1	1109	1110	1113.2	37.01	2.01	1105.2	27.58	4.25	1103.2	19.10	9.14	1126.8	14.44	7.67
ν_{60}	δHCC in ring 1	1128	1130	1142.1	83.04	11.32	1128.2	57.31	7.49	1118.1	97.45	6.21	1145.1	87.74	7.56
ν_{61}	δHCC in ring 2+$\nu O_{14}C_{16}$	1156	1156	1152.1	220.89	54.20	1141.7	94.54	26.05	1143.4	43.34	13.32	1165.1	60.81	11.74
ν_{62}	νC-CH_3+ρCH_3	1174	1172	1180.7	2.94	8.94	1173.9	2.95	8.44	1173.9	297.26	4.68	1202.1	14.15	7.20
ν_{63}	νC-CH_3+ρCH_3+δHCC in ring 2	-	-	1182.9	96.06	28.09	1177.8	3.02	8.85	1178.0	1.04	8.09	1205.6	261.50	4.26
ν_{64}	$\nu O_{14}C_{16}$+δHCC in ring 2 and 1+ νC-CH_3+ρCH_3	-	-	1184.5	382.18	51.38	1183.8	553.82	80.25	1181.3	2.60	8.63	1206.7	4.41	8.26
ν_{65}	δHCC in ring 1 and 2+δHOC	-	1201	1195.6	107.43	0.44	1188.0	43.08	8.33	1200.7	296.73	51.35	1213.3	333.33	41.78
ν_{66}	$\nu O_{12}C_4$+[δHCC+νCC] in ring 1+νC_3C_{11}	1210	-	1234.0	239.49	73.73	1234.3	252.80	65.37	1225.9	301.05	62.25	1249.3	253.41	56.94
ν_{67}	$\nu C_{23}C_{26}$+ρCH_3	1247	1243	1240.0	14.17	6.17	1236.6	156.79	25.92	1243.3	51.74	16.04	1267.7	32.91	9.17
ν_{68}	$\nu O_{12}C_4$+$\nu C_{11}C_3$+ [νCC+δHCC+δCCC] in ring 2 and 1	1264	1266	1279.2	173.61	4.87	1267.4	0.31	1.89	1259.9	2.56	7.90	1279.2	2.28	5.55
ν_{69}	[νCC+δHCC+δCCC] in ring 2 and 1+ νC_3C_{11}+$\nu O_{12}C_4$	1286	1287	1282.6	151.29	14.45	1281.4	263.69	3.26	1266.8	1.77	0.78	1298.0	0.49	1.43
ν_{70}	δHCC in ring 2	-	-	1290.4	1.09	0.85	1294.4	8.25	2.50	1279.4	331.44	5.32	1305.4	331.68	4.87
ν_{71}	[νCC+δHCC] in ring 1+νC_3C_{11}+$\nu O_{12}C_4$	1304	1307	1313.0	54.01	105.19	1321.2	121.60	133.55	1304.2	160.86	118.65	1326.2	150.84	110.05
ν_{72}	δCH_3 (sym. bending)	1320	1320	1353.1	8.84	0.13	1330.1	11.02	0.11	1326.4	12.08	0.10	1362.9	14.16	0.27
ν_{73}	δCH_3 (sym. bending)	1335	1331	1354.2	9.50	0.44	1331.2	12.46	0.69	1329.3	13.67	0.58	1363.8	13.10	0.01
ν_{74}	δHOC+[δHCC+νCC] in ring 1	1364	1362	1368.4	113.65	60.55	1361.2	8.20	1.96	1335.1	194.76	71.83	1377.4	166.41	69.75
ν_{75}	δCH_3 (sym. bending)	-	-	1384.4	4.16	0.84	1362.9	115.01	50.06	1358.9	5.12	0.71	1392.6	5.97	0.50
ν_{76}	[νCC+δHCC] in ring 2+ δCH_3 (sym. bending)	1395	1396	1388.7	5.65	0.30	1378.7	5.23	0.35	1381.2	6.40	0.64	1409.7	5.86	0.17

ν_{77}	$\delta_s CH_3$	-	-	1434.8	0.03	0.62	1411.2	0.03	0.59	1408.2	0.05	1.35	1439.1	0.00	1.14
ν_{78}	[νCC+δHCC] in ring 1	-	-	1439.4	41.32	52.68	1416.6	0.09	8.92	1410.9	0.08	7.54	1443.3	0.11	8.12
ν_{79}	$\delta_s CH_3$	-	-	1440.0	0.03	8.91	1419.4	1.50	9.31	1416.3	0.91	8.60	1447.6	0.99	8.51
ν_{80}	$\delta_s CH_3$	-	1445	1442.5	1.28	8.86	1433.1	35.86	54.06	1430.4	12.57	6.92	1461.5	12.00	7.34
ν_{81}	$\delta_s CH_3$	-	-	1455.2	12.60	6.97	1433.3	9.28	9.42	1434.2	23.45	40.21	1463.4	35.86	43.19
ν_{82}	$\delta_s CH_3$	1463	1462	1460.0	8.56	7.81	1437.7	8.97	8.01	1435.7	9.04	6.98	1465.5	9.04	8.16
ν_{83}	[νCC+δHCC] in ring 1+δHOC	-	-	1465.6	79.18	1.28	1449.8	6.05	3.32	1448.1	6.47	3.41	1477.1	8.38	2.36
ν_{84}	$\delta_s CH_3$	1483	-	1471.2	6.34	2.77	1455.4	103.58	2.19	1454.3	110.08	14.58	1485.7	95.08	4.44
ν_{85}	[νCC+δHCC] in ring 2	1510	1510	1489.2	93.29	0.68	1477.6	98.82	0.63	1482.6	114.80	0.82	1512.5	103.95	0.53
ν_{86}	[νCC+δHCC] in ring 1+δHOC	-	-	1563.4	62.99	27.98	1562.0	68.53	30.67	1568.2	68.31	38.55	1598.5	66.54	33.49
ν_{87}	[νCC+δHCC] in ring 2	1585	1586	1571.6	2.48	4.97	1570.3	2.66	4.51	1581.2	3.01	4.37	1609.8	2.57	5.28
ν_{88}	[νCC+δHCC] in ring 2 and 1	1602	1601	1588.8	19.00	78.86	1587.9	23.43	81.79	1601.1	37.02	95.56	1628.1	32.24	66.66
ν_{89}	[νCC+δHCC] in ring 1 and 2+δHOC	1616	1615	1599.2	39.91	10.30	1597.5	40.08	7.27	1607.5	32.73	7.40	1636.3	33.60	8.00
ν_{90}	νO=C+δHOC+νCC in ring 1	1689	1681	1665.6	330.03	181.26	1669.1	327.52	176.99	1699.6	342.85	173.19	1709.6	360.72	147.66
ν_{91}	$\nu_s CH_3$	2869	2872	2921.5	27.29	10.92	2900.6	26.77	9.91	2883.8	20.55	28.88	2944.1	23.25	9.06
ν_{92}	$\nu_s CH_3$	2900	2905	2922.0	26.85	7.97	2901.7	26.32	8.75	2886.1	22.75	46.36	2944.4	22.62	7.55
ν_{93}	$\nu_s CH_3$	-	2932	2929.3	28.73	516.33	2907.4	27.82	521.18	2891.3	14.90	400.26	2951.2	22.20	476.11
ν_{94}	$\nu_{as} CH_3$	-	-	2981.6	3.42	17.61	2970.1	3.23	17.67	2956.4	2.30	18.56	3008.1	4.03	15.86
ν_{95}	$\nu_{as} CH_3$	-	-	2982.4	3.23	15.61	2971.1	2.77	13.33	2958.0	5.41	22.55	3009.1	6.47	25.63
ν_{96}	$\nu_{as} CH_3$	2969	2968	2988.3	21.24	32.99	2975.3	19.56	35.69	2961.3	17.44	42.95	3014.6	15.11	24.57
ν_{97}	$\nu_{as} CH_3$	-	-	2989.8	100.46	261.47	2976.9	95.06	259.11	2962.2	46.54	145.92	3016.6	85.05	222.48
ν_{98}	$\nu_{as} CH_3$	-	-	2994.1	20.12	40.99	2980.9	22.48	43.79	2964.4	20.66	45.96	3019.7	21.04	43.46
ν_{99}	$\nu_{as} CH_3$	-	-	2996.6	42.93	64.94	2983.8	32.21	55.00	2969.0	38.28	109.35	3022.1	34.94	57.85
ν_{100}	νCH in ring 1	3023	-	3065.4	5.36	88.24	3045.2	5.27	86.90	3029.7	3.76	90.44	3086.2	4.57	84.02
ν_{101}	νCH in ring 2	-	3068	3072.9	11.54	41.46	3050.3	11.59	45.26	3031.2	5.66	36.53	3091.0	9.90	40.41
ν_{102}	νCH in ring 1	3073	-	3083.9	9.10	120.46	3063.4	5.91	52.51	3045.0	2.29	106.94	3103.1	4.23	59.57
ν_{103}	νCH in ring 2	-	-	3084.1	5.51	60.39	3063.9	6.95	114.33	3049.9	2.99	102.02	3105.0	6.22	107.65
ν_{104}	νCH in ring 2	-	-	3089.3	6.67	109.03	3068.7	5.10	101.70	3051.1	2.56	48.41	3109.1	3.99	102.89
ν_{105}	νCH in ring 1	-	-	3092.3	6.30	181.09	3072.5	5.00	155.10	3063.8	0.81	36.63	3113.4	3.41	150.82
ν_{106}	νCH in ring 2	-	-	3102.4	4.42	121.66	3079.0	3.67	131.79	3065.6	1.25	112.94	3122.1	2.86	118.64
ν_{107}	νCH in ring 1	-	-	3104.3	3.76	140.17	3081.7	4.32	164.32	3066.4	2.00	229.27	3123.6	3.14	149.11
ν_{108}	νOH	3207	3208	3353.0	416.37	141.80	3286.9	464.78	146.35	3424.6	393.18	133.08	3401.3	440.23	127.81
The linear correlation coefficients (R^2)				0.99916 for IR wavenumbers and 0.99930 for Raman ones			0.99951 for IR wavenumbers and 0.99961 for Raman ones			0.99916 for IR wavenumbers and 0.99836 for Raman ones			0.99909 for IR wavenumbers and 0.99927 for Raman ones		

ν, stretching; δ, in-plane bending; τ, torsion; γ, out-of-plane bending; δ_s, scissoring; δ_s, symmetric bending; ρ, rocking; I_{IR}, IR intensity (km/mol); S_{Raman}, Raman scattering activity.

3.3. NMR chemical shift analyses

The experimental (AIST, 2017) ^{1}H and ^{13}C NMR chemical shifts of the title molecule were measured in chloroform-d solvent. The ^{1}H and ^{13}C NMR chemical shifts of the title molecule were calculated at B3LYP, B3PW91, M06-2X and CAM-B3LYP/6-311++G(d,p) levels in vacuum and chloroform solvent with IEFPCM solvent model using GIAO method. The experimental and calculated NMR chemical shift values were listed in Table 3. The linear correlation coeffections (R^2) between the experimental and calculated proton and carbon-13 NMR chemical shifts were also given in Table 3.

Table 3. The experimental (AIST, 2017) and calculated ^{13}C and ^{1}H NMR isotropic chemical shifts (with respect to TMS, all values in ppm) of p-tert-butylphenyl salicylate.

Atoms	$\delta_{exp.}$	B3LYP		B3PW91		M06-2X		CAM-B3LYP	
		vacuum	chloroform	vacuum	chloroform	vacuum	chloroform	vacuum	chloroform
C1	119.43	123.39	124.87	122.29	123.78	138.19	139.85	124.79	126.31
C2	130.37	137.24	138.05	136.07	136.92	151.95	152.83	140.35	141.19
C3	111.98	117.47	117.92	115.55	116.01	129.58	129.95	118.03	118.53
C4	162.26	173.10	172.85	170.74	170.52	185.29	184.95	175.15	174.84
C5	117.84	123.93	124.17	122.99	123.27	138.87	139.13	125.79	125.99
C6	136.39	142.52	144.06	141.59	143.15	158.39	160.09	145.85	147.38
C11	169.14	177.01	178.17	174.90	176.01	183.64	184.69	179.34	180.55
C16	147.81	157.49	157.34	155.15	155.04	168.31	168.26	158.63	158.47
C17	120.98	127.19	127.55	126.25	126.69	140.88	141.51	130.22	130.55
C18	120.98	128.87	128.88	127.91	127.97	144.21	144.15	131.16	131.27
C19	126.53	134.86	135.97	133.86	134.99	150.4	151.64	137.22	138.30
C21	126.53	131.03	131.94	130.16	131.08	145.95	146.79	133.58	134.51
C23	149.30	157.46	159.19	155.15	156.92	173.74	175.63	159.62	161.36
C26	34.55	42.28	42.94	39.73	40.42	41.35	42.01	38.96	39.61
C27	31.41	34.56	34.67	34.03	34.16	35.72	35.79	34.41	34.51
C31	31.41	34.78	34.85	34.22	34.30	36.17	36.19	34.39	34.45
C35	31.41	30.22	30.39	29.69	29.87	33.51	33.61	30.52	30.70
R^2		**0.99824**	**0.99840**	**0.99875**	**0.99888**	**0.99564**	**0.99534**	**0.99894**	**0.99907**
H7	6.96	6.97	7.15	6.99	7.19	7.72	7.91	7.03	7.21
H8	8.07	8.35	8.44	8.38	8.49	9.07	9.16	8.51	8.60
H9	7.03	7.18	7.26	7.20	7.29	7.93	8.00	7.30	7.37
H10	7.52	7.61	7.80	7.64	7.84	8.16	8.34	7.73	7.91
H15	10.56	10.95	10.90	11.34	11.31	10.92	10.88	10.96	10.91
H20	7.13	7.32	7.43	7.36	7.49	7.97	8.09	7.42	7.52
H22	7.13	7.24	7.32	7.28	7.38	8.09	8.15	7.36	7.45
H24	7.46	7.61	7.75	7.68	7.84	8.34	8.49	7.79	7.93
H25	7.76	7.61	7.73	7.68	7.82	8.38	8.49	7.65	7.77
H28	1.34	1.62	1.65	1.63	1.68	1.63	1.66	1.66	1.68
H29	1.34	1.30	1.35	1.30	1.36	1.30	1.35	1.17	1.21
H30	1.34	1.21	1.18	1.22	1.20	1.24	1.19	1.29	1.24
H32	1.34	1.16	1.14	1.17	1.16	1.07	1.03	1.17	1.13
H33	1.34	1.32	1.36	1.29	1.35	1.34	1.39	1.29	1.33
H34	1.34	1.60	1.63	1.62	1.67	1.50	1.52	1.59	1.61
H36	1.34	1.61	1.63	1.62	1.66	1.51	1.53	1.55	1.57
H37	1.34	1.64	1.65	1.67	1.69	1.54	1.55	1.59	1.59
H38	1.34	1.09	1.14	1.10	1.16	1.40	1.45	1.15	1.19
R^2		**0.99721**	**0.99748**	**0.99622**	**0.99699**	**0.99587**	**0.99449**	**0.99732**	**0.99736**

^{13}C NMR chemical shifts were recorded in the interval of 31.41-169.14 ppm and they were computed in the region of 30.22-178.17 ppm for B3LYP, 29.69-176.01 ppm for B3PW91, 33.51-184.69 ppm for M06-2X and 30.52-180.55 ppm for CAM-B3LYP. Carbonyl carbons in esters, carboxylic acids, amides, ketones, phenols and aldehydes have characteristic chemical shift signals at the interval of 160-220 ppm, as the highly electronegative O atom reduces the electron density of carbon atom. But, the aromatic carbons occur signals in the region of 100-150 ppm (Anderson et al., 2004; Wade, 2006; Pavia et al., 2009). The NMR chemical shift signals for the C4 phenolic

carbon atom and C11 ester atom were recorded at 162.26 ppm and 169.14 ppm, respectively. The computed values for these carbon atoms are 173.10/172.85 ppm and 177.01/178.17 ppm for B3LYP, 170.74/170.52 ppm and 174.90/176.01 ppm for B3PW91, 185.29/184.95 ppm and 183.64/184.69 ppm for M06-2X and 175.15/174.84 ppm and 179.34/180.55 ppm for CAM-B3LYP, respectively. As expected, the other aromatic carbons were recorded in the region of 111.98-149.30 ppm, while they were calculated at the interval of 117.47-159.19 ppm, 115.55-156.92 ppm, 129.58-175.63 ppm and 118.03-161.36 ppm for aforementioned computation levels, respectively. Methyl and methylene carbon atoms are shielded by their own hydrogen atoms. Therefore, ^{13}C NMR resonance signals of these groups occur within the region of 15-35 ppm (Silverstein and Webster, 1998; Anderson et al., 2004; Stuart, 2004; Wade, 2006). The signals recorded at 31.41 ppm and 34.55 ppm in the Carbon-13 NMR isotropic chemical shift spectrum of the title molecule indicated presence of methyl groups (C26, C27, C31 and C35). The computed values corresponding to these carbon atoms were given in Table 3.

Due to intramolecular hydrogen bonding, phenolic protons shift to the approximate range of δ 10-12 ppm (Silverstein and Webster, 1998). The NMR chemical shift value for the phenolic H15 proton is observed at 10.56 ppm, while the computed values for this proton are between 10.90 ppm and 11.34 ppm in all mentioned computational levels. Aromatic hydrogens are deshielded at a higher level than those attached to double bonds due to the large anisotropic field that is generated by the circulation of the π electrons in the ring and they are easily identified in the region of 6.5-9.0 ppm (Pavia et al., 2009). The aromatic protons (H7, H8, H9 and H10) were experimentally recorded at the interval of 6.96-8.07 ppm, while they were theoretically computed at the regions of 6.97-8.44 ppm for B3LYP, 6.99-8.49 ppm for B3PW91, 7.72-9.16 ppm for M06-2X and 7.03-8.60 ppm for CAM-B3LYP. The methyl hydrogen atoms, shielded at the highest level, have chemical shift signals in the region of 0.7-1.3 ppm (Pavia et al., 2009). The methyl protons in the title molecule were experimentally and theoretically obtained at 1.34 ppm and at the interval of 1.09-1.68 ppm with the mentioned computational levels, respectively.

3.4. Frontier molecular orbitals analyses

The highest occupied molecular orbital (HOMO) and the lowest unoccupied molecular orbital (LUMO) are the main orbitals taking part in a chemical reaction (Fukui, 1982). The HOMO is the outermost orbital filled by electrons. It is represented by the ionization potential of a molecule. It can be considered as a valance band since it behaves as an electron donor. The LUMO represents the first empty innermost orbital unfilled by electrons. It is directly related to the electron affinity. Behaving as an electron acceptor, it can be thought as the conductance band of the system. The HOMO-LUMO energy band gap is an indication of molecular chemical stability. It is a very important parameter for determination of molecular electrical properties. Furthermore, the quantum molecular descriptors such as ionization potential, electron affinity, chemical reactivity, kinetic stability, polarizability, chemical hardness and softness, aromaticity and electronegativity can be found using HOMO-LUMO energy band gap (Alpaslan et al., 2015). HOMO and LUMO energy values and HOMO-LUMO band gap values, computed with the B3LYP, B3PW91, M06-2X and CAM-B3LYP/6-311++G(d,p) levels, were summarized in Table 4. Additionally, the ionization potential, chemical potential, electron affinity, electronegativity chemical hardness, softness and electrophilicity index parameters, found using the computed HOMO and LUMO energy values, were summarized in Table 4 (Alpaslan et al., 2015). HOMO and LUMO surfaces were given in Figure 4. As seen from Figure 4, both HOMO and LUMO plots simulated with all four-computational level were localized on salicylate group of p-tert-butylphenyl salicylate molecule.

Table 4. The calculated molecular electronic properties of p-tert-butylphenyl salicylate (vacuum/ethanol).

Parameters (eV)	B3LYP	B3PW91	M06-2X	CAM-B3LYP
E_{LUMO}	-1.8090/-1.9421	-1.8117/-1.9638	-0.8177/-0.9557	-0.5021/-0.6416
E_{HOMO}	-6.5686/-6.7218	-6.5914/-6.7658	-7.9003/-8.0584	-7.9572/-8.1275
Energy band gap $\lvert E_{HOMO}\text{-}E_{LUMO}\rvert$	4.7595/4.7797	4.7797/4.8020	7.0826/7.1027	7.4551/7.4859
Ionization potential ($I = -E_{HOMO}$)	6.5686/6.7218	6.5914/6.7658	7.9003/8.0584	7.9572/8.1275
Electron affinity ($A = -E_{LUMO}$)	1.8090/1.9421	1.8117/1.9638	0.8177/0.9557	0.5021/0.6416
Chemical hardness ($\eta = (I-A)/2$)	2.3798/2.3898	2.3898/2.4010	3.5413/3.5514	3.7276/3.7429
Chemical softness ($\zeta = 1/2\eta$)	0.2101/0.2092	0.2092/0.2082	0.1412/0.1408	0.1341/0.1336
Electronegativity ($\chi = (I+A)/2$)	4.1888/4.3319	4.2016/4.3648	4.3590/4.5070	4.2296/4.3846
Chemical potential ($\mu = -(I+A)/2$)	-4.1888/-4.3319	-4.2016/-4.3648	-4.3590/-4.5070	-4.2296/-4.3846
Electrophilicity index ($\omega = \mu^2/2\eta$)	3.6865/3.9261	3.6934/3.9675	2.6828/2.8599	2.3996/2.5681

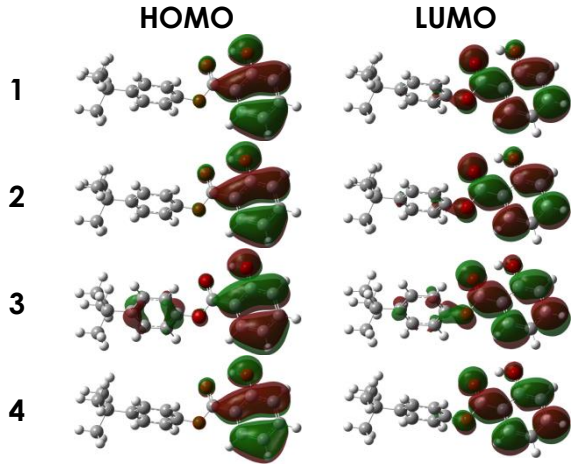

Figure 4. The HOMO and LUMO plots of p-tert-butylphenyl salicylate (**1**= B3LYP, **2**= B3PW91, **3**= M06-2X and **4**= CAM-B3LYP).

3.5. NBO analysis

NBO analysis is a powerful method to determine intra-molecular and inter-molecular bonding interactions, bond species, bond structures and hyperconjugation interactions in molecular systems. The stabilization energy, $E(2)$, depends on the interaction between Lewis type (bonding or lone pair) filled orbitals and non-Lewis type (antibonding or Rydberg) vacancy orbitals. For each donor NBO (i) and acceptor NBO (j), the stabilization energy $E(2)$ associated with the electron delocalization between stabilization energy $E(2)$ associated with the electron delocalization between the donor and the acceptor is estimated as (Wienhold and Landis, 2005);

$$E(2) = -q_i \frac{F_{ij}^{\ 2}}{\Delta E} = -q_i \frac{\langle i|F|j\rangle^2}{\varepsilon_j - \varepsilon_i}$$

Where q_i is the donor orbital occupancy, ε_i and ε_j are diagonal elements (orbital energies), and F_{ij} is the off-diagonal NBO Fock matrix element. Table 5 shows the results of second-order perturbation theory analysis of the Fock Matrix computed with B3LYP, B3PW91, M06-2X and CAM-B3LYP/6-311++G(d,p) levels for the intra-molecular O-H···O interaction in the title molecule. According to the computed NBO results, the n(O13)→σ*(O12-H15) charge transfer for the intramolecular hydrogen bonding in the title molecule belongs to the stabilization energy of 17.24 kcal mol^{-1} for B3LYP, 19.69 kcal mol^{-1} for B3PW91, 14.85 kcal mol^{-1} for M06-2X and 19.92 kcal mol^{-1} for CAM-B3LYP.

Table 5. The calculated results with second order perturbation theory of Fock matrix in NBO of p-tert-butylphenyl salicylate.

Method	ED(i)(e)	Donor (i)	ED(j)(e)	Acceptor (j)	E(2)[a] (kcal/mol)	E(j)-E(i)[b] (a.u.)	F(i,j)[c] (a.u.)
B3LYP	1.97154	n(O13)	0.04433	σ*(O12-H15)	3.17	1.13	0.054
	1.83711	n(O13)	0.04433	σ*(O12-H15)	14.07	0.71	0.092
B3PW91	1.97112	n(O13)	0.04914	σ*(O12-H15)	3.63	1.13	0.057
	1.83281	n(O13)	0.04914	σ*(O12-H15)	16.06	0.72	0.099
M06-2X	1.97339	n(O13)	0.03336	σ*(O12-H15)	3.14	1.31	0.057
	1.85046	n(O13)	0.03336	σ*(O12-H15)	11.71	0.87	0.093
CAM-B3LYP	1.97088	n(O13)	0.04277	σ*(O12-H15)	3.92	1.27	0.063
	1.84407	n(O13)	0.04277	σ*(O12-H15)	16.00	0.85	0.107

ED is the electron density.
[a] E(2) is the energy of hyperconjugative interactions.
[b] Energy difference between donor (i) and acceptor (j) NBO.
[c] F(i,j) is the Fock matrix element between i and j NBO.

3.6. NLO analysis

Organic, inorganic and organometallic nonlinear optical (NLO) materials have drawn much interest in the fields of physics, chemistry and engineering, due to their potential for future applications in the fields of optoelectronics and microelectronics, such as optical telecommunications, signal processing, optical interconnections, optical computing, optical information processing, sensor protection, optical switching, dynamic image processing and various other photonic technologies (Nalwa and Miyata, 1997). Mean polarizability (α_{total}), anisotropy of polarizability ($\Delta\alpha$) and first hyperpolarizability (β_0) values are important factors to determine NLO properties of molecular systems. Therefore, recent syntheses and investigations of novel nonlinear optic materials with high performance have created an interesting study area.

Dipole moments, polarizabilities and the first hyperpolarizabilities of the title molecule were computed with B3LYP, B3PW91, M06-2X and CAM-B3LYP functionals at the 6-311++G(d,p) basis set by using the finite-field approach and they were summarized in Table 6. Total dipole moment (μ_{total}), mean polarizability (α_{total}), anisotropy of the polarizability ($\Delta\alpha$) and the first hyperpolarizability

Table 6. The computed dipole moments, polarizability and first hyperpolarizability values of p-tert-butylphenyl salicylate.

Parameters	B3LYP	B3PW91	M06-2X	CAM-B3LYP
α_{xx}	45.857057	45.473318	43,918975	43.590784
α_{xy}	-1.468724	-1.447369	-1,205952	-1.491938
α_{xz}	0.449402	0.475443	0.498052	0.270501
α_{yy}	27.495369	27.189745	27.844298	26.498934
α_{yz}	0.469464	0.481560	0.619328	0.309205
α_{zz}	23.023234	22.626691	21.211417	22.961580
α_{total}	32.125220	31.763251	30.991563	31.017099
$\Delta\alpha$	21.142517	21.123398	20.378165	19.294768
μ_x	-1.4442	-1.4885	-1.4025	-1.5652
μ_y	-1.6647	-1.6355	-2.0823	-1.7500
μ_z	0.7754	0.7834	0.4717	0.6313
μ_{total}	2.3363	2.3461	2.5545	2.4312
β_{xxx}	-55.968084	-52.625296	-46.395861	-57.108908
β_{xyy}	4.261637	4.600238	3,859765	5.394967
β_{xzz}	-2.829172	2.527659	1,929119	3.227416
β_{yyy}	-17.457290	-16.207580	-16.276324	-16.228853
β_{yxx}	14.480956	14.150298	15.123341	12.616432

β_{yzz}	-6.695821	-6.313197	-5,074227	-6.136804
β_{zzz}	3.084199	2.925735	4,045505	1.341176
β_{zxx}	-2.916310	-2.832231	-3,601204	-1.264909
β_{zyy}	1.153410	1.220107	0.722601	1.530175
β_0	55.402438	46.279626	41.098253	49.463611

$\times 10^{-24}$ for α in esu, $\times 10^{-31}$ for β in esu, μ in Debye, 1 a.u.= 0.1482×10^{-24} for α in esu and 1 a.u.= 8.6393×10^{-33} for β in esu

(β_0) magnitudes were computed using the following equations (Temel et al., 2015);

$$\alpha_{total} = \frac{1}{3}(\alpha_{xx} + \alpha_{yy} + \alpha_{zz})$$

$$\Delta\alpha = \frac{1}{\sqrt{2}}\left[\begin{array}{l}(\alpha_{xx} - \alpha_{yy})^2 + (\alpha_{yy} - \alpha_{zz})^2 + (\alpha_{zz} - \alpha_{xx})^2 \\ + 6\alpha_{xz}{}^2 + 6\alpha_{xy}{}^2 + 6\alpha_{yz}{}^2\end{array}\right]^{\frac{1}{2}}$$

$$\beta_0 = \left[\begin{array}{l}(\beta_{xxx} + \beta_{xyy} + \beta_{xzz})^2 + (\beta_{yyy} + \beta_{yzz} + \beta_{yxx})^2 \\ + (\beta_{zzz} + \beta_{zxx} + \beta_{zyy})^2\end{array}\right]^{\frac{1}{2}}$$

$$\mu_{total} = (\mu_x^2 + \mu_y^2 + \mu_z^2)^{\frac{1}{2}}$$

The calculated dipole moment (μ_{total}) values for the title molecule were found as 2.3363 Debye for B3LYP, 2.3461 Debye for B3PW91, 2.5545 Debye for M06-2X and 2.4312 Debye for CAM-B3LYP. The α_{total}, $\Delta\alpha$ and β_0 values were computed as 32.125220×10^{-24}, 21.142517×10^{-24} and 55.402438×10^{-31} esu for B3LYP, 31.763251×10^{-24}, 21.123398×10^{-24} and 46.279626×10^{-31} esu for B3PW91, 30.991563×10^{-24}, 20.378165×10^{-24} and 41.098253×10^{-31} esu for M06-2X and 31.017099×10^{-24}, 19.294768×10^{-24} and 49.463611×10^{-31} esu for CAM-B3LYP, respectively. Urea that is the most common organic NLO material can be usually compared with those of other organic compounds. By using B3LYP/6-311++G(d,p) level, computed values for urea are 5.047959×10^{-24} esu for α_{total}, 2.036631×10^{-24} esu for $\Delta\alpha$ and 7.878196×10^{-31}esu for β_0. The α_{total}, $\Delta\alpha$ and β_0 values calculated with B3LYP/6-311++G(d,p) level of the title compound are approximately 6.364, 10.381 and 7.324 times greater than those of urea, respectively.

3.7. Thermodynamic properties

The thermodynamic parameters were calculated using B3LYP, B3PW91 and CAM-B3LYP methods with the 6-311++G(d,p) basis set at the room temperature of 298.15 K, under 1 atm pressure and in vacuum for the title molecule. The computed thermodynamic parameters were given in Table 7. The partition function, indicating the statical properties of a system in thermodynamic equilibrium is very important for thermodynamic parameters. There are four types of partition functions, namely, translational, electronic, vibrational and rotational partition functions. Partition functions can be used to compute the thermodynamic variables (such as heat capacity, entropy, equilibrium constants, total energy, free energy, pressure, thermal energy and rate constants, etc.) of a system. As known, the total energy of any molecular system is the sum of electronic, vibrational, rotational and translation energies (or $E = E_e + E_v + E_r + E_t$). The computed total energy values for the title molecule were obtained as -884.59282006 Hartrees for B3LYP, -884.24252309 Hartrees for B3PW91, -884.22227194 Hartrees for M06-2X and -884.13686115 Hartrees for CAM-B3LYP. The computed zero-point vibrational energy (ZPVE) values for all four levels were found as 195.37107, 195.84427, 197.44399 and 197.70185 kcal/mol, respectively. As seen from Table 7, the computed thermal energy (E), heat capacity (C_v) and entropy (S) values for B3LYP, B3PW9, M06-2X and CAM-B3LYP/6-311++G(d,p) levels are 206.790, 207.257, 208.763 and 207.407 cal/mol×K, 71.656, 71.566, 71.003 and 68.641 cal/mol×K and 141.872, 141.859, 140.605 and 133.286 cal/mol×K, respectively. The major contributions to these values were from vibrational energies, whereas the minor contributions resulted from electronic, transitional and rotational energies. The computed rotational temperatures (Kelvin), rotational constants (GHz) and other thermodynamic parameters for the title molecule were listed in Table 7.

Table 7. The computed thermodynamic parameters (at the temperature of 298.15 K, under the pressure of 1 atm and in vacuum) of p-tert-butylphenyl salicylate.

Parameters	B3LYP	B3PW91	M06-2X	CAM-B3LYP
Thermal energy, E (cal/mol K)				
Electronic	0.000	0.000	0.000	0.000
Translational	0.889	0.889	0.889	0.889
Rotational	0.889	0.889	0.889	0.889
Vibrational	205.013	205.479	206.986	206.630
Total	206.790	207.257	208.763	207.407
Heatcapacity, C_v (cal/mol K)				
Electronic	0.000	0.000	0.000	0.000
Translational	2.981	2.981	2.981	2.981
Rotational	2.981	2.981	2.981	2.981
Vibrational	65.694	65.604	65.041	62.679
Total	71.656	71.566	71.003	68.641
Entropy, S (cal/mol K)				
Electronic	0.000	0.000	0.000	0.000
Translational	42.680	42.680	42.680	42.680
Rotational	34.185	34.164	34.166	34.152
Vibrational	65.007	65.014	63.759	56.454
Total	141.872	141.859	140.605	133.286
Rotational temperatures (Kelvin)				
A	0.05548	0.05580	0.05576	0.05598
B	0.00599	0.00604	0.00607	0.00606
C	0.00575	0.00579	0.00576	0.00583
Rotational constants (GHz)				
A	1.15611	1.16276	1.16182	1.16650
B	0.12490	0.12586	0.12649	0.12622
C	0.11978	0.12065	0.11996	0.12143
Zero-point vibrational energy (kcal/mol)	195.37107	195.84427	197.44399	197.70185
Zero-point correction*	0.311344	0.312098	0.314647	0.315058
Thermal correction to Energy*	0.329541	0.330285	0.332685	0.332118
Thermal correction to Enthalpy*	0.330485	0.331229	0.333629	0.333063
Thermal correction to Gibbs Free Energy*	0.263077	0.263827	0.266824	0.269734
Sum of electronic and zero-point energy*	-884.281476	-883.930425	-883.907625	-883.821803
Sum of electronic and thermal Energies*	-884.263279	-883.912238	-883.889587	-883.804743
Sum of electronic and thermal Enthalpies*	-884.262335	-883.911294	-883.888643	-883.803799
Sum of electronic and thermal Free Energies*	-884.329743	-883.978696	-883.955448	-883.867127
Total energy (Hartree)	-884.59282006	-884.24252309	-884.22227194	-884.13686115

* in Hartree/particle

4. Conclusions

The molecular geometric, spectroscopic (FT-IR, Raman and NMR), HOMO-LUMO, NBO, NLO and thermodynamic analyses for p-tert-butylphenyl salicylate molecule were investigated using experimental and theoretical methods. In order to support the experimental spectroscopic data, theoretical computations were performed using B3LYP, B3PW91, M06-2X and CAM-B3LYP methods with the 6-311++G(d,p) basis set. The computed total molecular energy was obtained in the following order: B3LYP<B3PW91<M06-2X<CAM-B3LYP. As seen from the tables and figures, the computed structural, spectroscopic, electronic, nonlinear optical and thermodynamic properties varied depending on the calculation levels. In the present study, due to O-H···O intramolecular hydrogen bonding interaction in title compound, O-H vibrational frequencies, ^{1}H NMR isotropic chemical shifts for mentioned proton, and NBO analysis of n(O)→σ*(O-H) interaction were investigated using experimental and theoretical methods. The calculated α_{total}, $\Delta\alpha$ and β_0 values show that p-tert-butylphenyl salicylate molecule may be a good nonlinear optical material. The

thermodynamic parameters were computed to understand the thermochemical properties (at the room temperature of 298.15 K, under 1 atm pressure and in vacuum) of the title compound.

References

AIST, (2017). National Institute of Advanced Industrial Science and Technology Spectral Database for Organic Compounds, SDBS.http://sdbs.db.aist.go.jp/sdbs/cgibin/cre_index.cgi, (Accessed on 10 March 2017).

Alpaslan, Y.B., Gökce, H., Alpaslan, G., Macit, M. (2015). Spectroscopic Characterization and Density Functional Studies of (Z)-1-[(2-methoxy-5-(trifluoromethyl) phenylamino) methylene] naphthalene-2(1H)-one, Journal of Molecular Structure, 1097, 171-180.

Anderson, R.J., Bendell, D.J., Groundwater, P.W. (2004). Organic Spectroscopic Analysis, The Royal Society of Chemistry, Sanderland UK.

Baran, J., Davydova, N.A. (2010). Infrared spectroscopy study of structural changes in glass-forming salol, Physical Review E, 031503.1-6.

Becke, A.D. (1993). Density functional Thermochemistry. III. The Role of Exact Exchange. The Journal of Chemical Physics, 98, 5648-5652.

Bellamy, L.J. (1975). The Infrared Spectra of Complex Molecules, 3rd ed. Wiley, New York.

Bilgram, J.H., Dürig, U., Wächter. M., Seiler, P. (1982). Zone Refining and Structure Determination of Salol Crystals, Journal of Crystal Growth, 57, 1-5.

Buyukuslu, H., Akdogan, M., Yildirim, G., Parlak, C. (2010). Ab Initio Hartree-Fock and Density Functional Theory Study on Characterization of 3-(5-methylthiazol-2-yldiazenyl)-2-phenyl-1H-indole, Spectrochimica Acta Part A: Molecular and Biomolecular Spectroscopy, 75(4), 1362-1369.

Ceylan, Ü., Tarı, G.Ö., Gökce, H., Ağar, E. (2016). Spectroscopic (FT-IR and UV-Vis) and Theoretical (HF and DFT) Investigation of 2-Ethyl-N-[(5-nitrothiophene-2-yl) methylidene] aniline, Journal of Molecular Structure, 1110, 1-10.

Chase, H.M., Rudshteyn, B., Psciuk, B.T., Upshur, M.A., Strick, B.F., Thomson, R.J., Batista, V.S., Geiger, F.M. (2016). Assessment of DFT for Computing Sum Frequency Generation Spectra of an Epoxydiol and a Deuterated Isotopologue at Fused Silica/Vapor Interfaces, The Journal of Physical Chemistry B, 120(8), 1919-1927.

Choi, Y.H., Na, B.H., Choi, Y.S., Rahman, M.S., Kim, M.R., Jee, J., Shin, J., Suh, J.W., Yoo, J.C. (2016). Anti-inflammatory Function of 4-Tert-butylphenyl Salicylate Through Down-Regulation of the NF-kappa B Pathway, Archives of Pharmacal Research, 39(3), 429-436.

Colthup, N.B., Daly, L.H., Wiberley, E. (1964). Introduction to Infrared and Raman Spectroscopy, Academic Press, New York.

Dennington, R., Keith, T., Millam J. (Eds.). (2009). GaussView, Version 5, Semichem Inc., Shawnee Mission KS.

Ditchfield, R. (1974). Self-consistent Perturbation Theory of Diamagnetism. Molecular Physics, 27, 789-807.

Dobashi, Y., Ohkatsu, Y. (2008). Dependence of Ultraviolet Absorbers' Performance on Ultraviolet Wavelength, Polymer Degradation and Stability, 93(2), 436-447.

Frisch, M.J., Trucks, G.W., Schlegel, H.B., Scuseria, G.E., et al. (2009). Gaussian 09, Revision C.01, Gaussian, Inc., Wallingford CT.

Fukui, K. (1982). Role of Frontier Orbitals in Chemical Reactions, Science, 218, 747-754.

Gottfried, C., Dutzer, M.J. (1961). Status of Investigations for Improving Weatherability of Linear Polyethylene and Copolymers, Journal of Applied Polymer Science, 5(17), 612-619.

Hammond, R.B., Jones, M.J., Roberts, K.J., Kutzke, H., Klapper, H. (2002). A Structural Study of Polymorphism in Phenyl Salicylate: Determination of the Crystal Structure of a Meta-Stable Phase from X-Ray Powder Diffraction Data Using a Direct Space Systematic Search Method, Zeitschrift-fur-Kristallographie, 217(9), 484-491.

Hanuza, J., Sasiadek, W., Michalski, J., Lorenc, J.,

Maczka, M., Kaminskii, A.A., Butashin, A.V., Klapper, H., Hulliger, J., Mohmed, A.F.A. (2004). Polarized Raman and Infrared Spectra of the Salol Crystal-Chemical Quantum Calculations of the Vibrational Normal Modes, Vibrational Spectroscopy, 34(2), 253-268.

Hutchinson, E. (2003). An aspirin a day, Nature Reviews Cancer, 3(8), 552-552.

Kalampounias, A.G., Yannopoulos, S.N., Steffen, W., Kirillova, L.I., Kirillov, S.A. (2003). Short-time Dynamics of Glass-Forming Liquids: Phenyl Salicylate (Salol) in Bulk Liquid, Dilute Solution, and Confining Geometries, The Journal of Chemical Physics, 118(18), 8340-8349.

Kanagathara, N., Marchewka, M.K., Drozd, M., Gunasekaran, S., Rajakumar, P.R., Anbalagan, G. (2015). Structural and Vibrational SpectroscopicStudies on Charge Transfer andIonic Hydrogen Bonding Interactions of Melaminium Benzoate Dihydrate, Spectrochimica Acta Part A: Molecular and Biomolecular Spectroscopy, 145, 394-409.

Kasumov, V.T., Köksal, F. (2002). Synthesis, Spectroscopic Characterization and EPR Studies on Electron Transfer Reactions of Bis [N-(2,5-di-tert-butylphenyl) salicylaldiminato] copper Complexes with PPh 3, Spectrochimica Acta Part A: Molecular and Biomolecular Spectroscopy, 58(10), 2199-2211.

Kavitha, T., Velraj, G. (2016). Structural, Spectroscopic (FT-IR, FT-Raman, NMR) and Computational Analysis (DOS, NBO, Fukui) of 3,5-dimethylisoxazole and 4-(chloromethyl)-3,5-dimethylisoxazole: A DFT Study, Journal of Theoretical and Computational Chemistry, 15(05), 1650039.

Lee, C., Yang, W., Parr, R.G. (1988). Development of the Colle-Salvetti Correlation-Energy Formula into a Functional of the Electron Density, Physical Review B, 37, 785-789.

London, F. (1937). Théorie Quantique Des Courants Interatomiques Dans Les Combinaisons Aromatiques, Journal de Physique et le Radium, 8, 397-409.

Schmitt, R.G., Hirt, R.C. (1960). Investigation of the Protective Ultraviolet Absorbers in a Space Environment. I. Rate of Evaporation and Vapor Pressure Studies, Journal of Polymer Science Part A: Polymer Chemistry, 45(145), 35-47.

Madan, R.K., Levitt, J. (2014). A Review of Toxicity from Topical Salicylic Acid Preparations, Journal of The American Academy of Dermatology, 70(4), 788-792.

Nalwa, H.S., Miyata, S. (1997). Nonlinear Optics of Organic Molecules and Polymers, CRC Press, Boca Raton, FL.

Newland, G.C., Tamblyn, J.W. (1964). Mechanism of Ultraviolet Stabilization of Polymers by Aromatic Salicylates, Journal of Applied Polymer Science, 8(5), 1949-1956.

Nyquist, R.A., Putzig, C.L., Clark, T.L., McDonald, A.T. (1996). Infrared Study of Intramolecularly Hydrogen Bonded Aromatic Carbonyl Containing Compounds in Various Solvents, Vibrational Spectroscopy, 12(1), 93-102.

Ortiz, A.F.C., López, A.S., Ríos, A.G., Cabezas, F.C., Correa, C.E.R. (2015). Experimental and Theoretical Studies on the Structure and Spectroscopic Properties of (E)-1-(2-aminophenyl)-3-(pyridine-4-yl) prop-2-en-1-one, Journal of Molecular Structure, 1098, 216-228.

Öztürk, N., Gökce, H. (2017). Structural and Spectroscopic (FT-IR and NMR) Analyses on (E)-pent-2-enoic Acid, Bilge International Journal of Science and Technology Research, 1(1), 9-15.

Pavia, D.L., Lampman, G.M., Kriz, G.S., Vyvyan, J.R. (2009). Introduction to Spectroscopy, Brooks/Cole Cengage Learning, USA.

Perdew, J.P., Burke, K., Wang, Y. (1996). Generalized Gradient Approximation for the Exchange-Correlation Hole of a Many-Electron System, Physical Review B, 54(23), 16533.

Pubchem, (2017). U.S. National Library of Medicine, Open Chemistry Database, https://pubchem.ncbi.nlm.nih.gov/compound/4-tert-Butylphenyl_salicylate (Accessed on 10 March 2017).

Raja, G., Saravanan, K., Sivakumar, S. (2013). Structure and Vibrational Spectroscopic Studies of 1-Naphthol: Density Functional Theory Calculations, International Journal on Applied Bioengineering, 7(1), 45-56.

Silverstein, R.M., Webster, F.X. (1998). Spectroscopic Identification of Organic Compound, 6nd ed., John Willey & Sons, New York.

Stuart, B.H. (2004). Infrared Spectroscopy: Fundamentals and Applications, JohnWilley & Sons, England.

Temel, E., Alaşalvar, C., Gökçe, H., Güder, A., Albayrak, Ç., Alpaslan, Y.B., Alpaslan, G., Dilek, N. (2015). DFT Calculations, Spectroscopy and Antioxidant Activity Studies on (E)-2-nitro-4-[(phenylimino) methyl] phenol, Spectrochimica Acta Part A: Molecular and Biomolecular Spectroscopy, 136, 534-546.

Wade Jr, L.G. (2006). Organic Chemistry, Pearson Prentice Hall, New Jersey.

Wienhold, F., Landis, C.R. (2005). Valency and Bonding-A Natural Bond Orbital Donor-Acceptor Perspective, Cambridge University Press, New York.

Wolinski, K., Himton, J.F., Pulay, P. (1990). Efficient Implementation of the Gauge-Independent Atomic Orbital Method for NMR Chemical Shift Calculations, Journal of the American Chemical Society, 112, 8251-8260.

Yanai, T., Tew, D.P., Handy, N.C. (2004). A New Hybrid Exchange-Correlation Functional Using the Coulomb-Attenuating Method (CAM-B3LYP), Chemical Physics Letters, 393(1), 51-57.